Phenomenological analysis of the nucleon spin contents and their scale dependence

M. Wakamatsu and Y. Nakakoji

Department of Physics, Faculty of Science, Osaka University, Toyonaka, Osaka 560-0043, Japan

(Received 12 December 2007; published 17 April 2008)

In the past few years, a great deal of evidence has accumulated which indicates that the gluon polarization inside the nucleon is likely to be small at least at the low renormalization scales. On the other hand, the recent lattice QCD analyses suggest that the net orbital angular momentum carried by the quarks is nearly zero. There is also some indication, noted by Brodsky and Gardner based on the COMPASS observation of small single-spin asymmetry on the isoscalar deuteron target, that the gluon orbital angular momentum inside the nucleon is likely to be small. Naively combining all these observations, we are led to a rather embarrassing conclusion that the nucleon constituents altogether do not carry an adequate amount of angular momentum saturating the total nucleon spin. We show that this somewhat confused state of affairs can be cleared up only by paying careful attention to the scale dependencies of the nucleon spin decomposition.

DOI: 10.1103/PhysRevD.77.074011 PACS numbers: 12.39.Fe, 12.38.Lg, 12.39.Ki, 13.15.+g

I. INTRODUCTION

If the intrinsic quark spin carries a little of the total nucleon spin, what carries the rest of it? This is the famous ''nucleon spin problem'' raised by the EMC measurements nearly 20 years ago [1,2]. In the past few years, there have been several remarkable advances toward the resolution of this long-standing problem. First, a lot of experimental evidence has been accumulated, which indicates that the gluon polarization inside the nucleon is likely to be small, at least at the low renormalization scales [3–6]. At the least, it is now widely accepted that the $U_A(1)$-anomaly motivated explanation of the nucleon spin puzzle is disfavored. Second, the quark spin fraction or the net longitudinal quark polarization $\Delta\Sigma$ has been fairly precisely determined through the high-statistics measurements of deuteron spin structure function by the COMPASS [7,8] and HERMES groups [9]. According to their new analyses, the portion of the nucleon spin coming from the intrinsic quark spin is around 30%. Putting together these two observations blindly, one might be led to the conclusion that the rest of the nucleon spin must be carried by the orbital angular momentum of quarks and/or gluons. On the other hand, however, the recent lattice QCD simulations indicate that the net orbital angular momentum carried by the quark fields is very small or close to zero [10–18]. Besides, based on the conjecture on the relation between the Sivers mechanism and the quark and gluon orbital angular momenta [19,20], Brodsky and Gardner [21] argued that the small single-spin asymmetry observed by the COMPASS Collaboration on the deuteron target [22] is an indication of small gluon orbital angular momentum inside the nucleon.

Naively combining all the observations above, we might be led to the conclusion that the nucleon constituents on aggregate do not carry an adequate amount of angular momentum saturating the total nucleon spin. What's wrong with the above deduction? The purpose of the present study is to resolve the apparent paradox above. To clear up this confused status of our understanding of the nucleon spin puzzle, we propose to carry out an analysis, in which special care is paid to the fact that the decomposition of the nucleon spin is an absolutely scale-dependent idea. What plays a central role in this analysis is Ji's angular momentum sum rule, supplemented with some additional knowledge listed below. The first is the information obtained from the recent theoretical studies of the isoscalar and isovector combinations of the nucleon anomalous gravitomagnetic moments, $B_{20}^{u+d}(0)$ and $B_{20}^{u-d}(0)$, within the lattice QCD as well as within the chiral quark soliton model (CQSM). The second is the empirical information on the momentum fractions carried by the quarks and gluons, as well as on the longitudinal quark polarizations. The third is the observation, first made by Ji, that the total angular momentum fractions carried by the quarks and gluons obey exactly the same evolution equations as do the momentum fractions of the quarks and gluons.

The plan of the paper is as follows. First, in Sec. II, we briefly review main predictions of the lattice QCD simulations for generalized form factors and the spin contents of the nucleon carried out in the past few years. On the other hand, Sec. III is devoted to new and improved investigation of the corresponding generalized form factors within the framework of the chiral quark soliton model. Next, in Sec. IV, armed with the knowledge gained in the previous two sections, we try to carry out semiempirical analysis of the nucleon spin contents by paying special attention to their scale dependence. Several concluding remarks will then be given in Sec. V.

II. LATTICE QCD PREDICTIONS ON NUCLEON SPIN CONTENTS

Most theoretical analyses of the nucleon spin contents nowadays heavily rely upon Ji's angular momentum sum rule [23–26]. According to it, the total angular momentum

carried by the quark field with flavor q is given as

$$J^q = \frac{1}{2}[A^q_{20}(0) + B^q_{20}(0)] = \frac{1}{2}[\langle x\rangle^q + B^q_{20}(0)]. \quad (1)$$

Here, $A^q_{20}(0)$ is the forward ($t \to 0$) limit of the generalized Dirac form factor $A^q_{20}(t)$, which is related to the second moment of the unpolarized spin-non-flip generalized parton distribution function (GPD) $H^q(x, \xi, t)$. It just reduces to the momentum fraction $\langle x\rangle^q$ carried by the quark with flavor q. On the other hand, $B^q_{20}(0)$ is the forward limit of the generalized Pauli form factor $B^q_{20}(t)$, which is sometimes called the anomalous gravitomagnetic moment (AGM). (More precisely, $B^q_{20}(0)$ is the contribution of the quark with flavor q to the nucleon AGM.) The quantity $B^q_{20}(0)$ is also related to the second moment of the unpolarized spin-flip generalized parton distribution $E^q(x, \xi, t)$, so that it is in principle measurable through the high-energy deeply virtual Compton scatterings (DVCS) and/or deeply virtual meson production processes [23,26]. Confining to the two-flavor case, for simplicity, we have two independent relations:

$$J^{u+d} = \frac{1}{2}[\langle x\rangle^{u+d} + B^{u+d}_{20}(0)], \quad (2)$$

$$J^{u-d} = \frac{1}{2}[\langle x\rangle^{u-d} + B^{u-d}_{20}(0)]. \quad (3)$$

Since the quark momentum fractions $\langle x\rangle^{u+d}$ and $\langle x\rangle^{u-d}$ are empirically known fairly well, the knowledge of $B^{u+d}_{20}(0)$ and $B^{u-d}_{20}(0)$ is essential to extract the total angular momentum J^u and J^d carried by the u- and d-quarks. In fact, these are the quantities of central interest in several lattice QCD studies [10–18]. Here, we briefly review the relevant predictions of lattice QCD studies on the nucleon spin contents in the past few years.

We first look into the results on $B^{u+d}_{20}(0)$ and $B^{u-d}_{20}(0)$ reported by the QCDSF Collaboration in [10,11] some years ago. Their predictions are

$$\begin{aligned} B^{u+d}_{20}(0) &= 0.102 \pm 0.113, \\ B^{u-d}_{20}(0) &= 0.566 \pm 0.113. \end{aligned} \quad (4)$$

(We recall that their simulations were performed in the so-called heavy-pion region with $m_\pi \simeq (640\text{–}1070)$ MeV. The values quoted in (4) are those extrapolated to the physical pion mass. In practice, however, no strong pion mass dependencies were observed in their simulations at this stage.) Combining (4) with their predictions on $A^{u+d}_{20}(0)$ and $A^{u-d}_{20}(0)$, given by

$$\begin{aligned} A^{u+d}_{20}(0) &= \langle x\rangle^{u+d} = 0.547 \pm 0.022, \\ A^{u-d}_{20}(0) &= \langle x\rangle^{u-d} = 0.253 \pm 0.022, \end{aligned} \quad (5)$$

they estimated that

$$2J^u = 0.74 \pm 0.12, \qquad 2J^d = -0.08 \pm 0.08. \quad (6)$$

Further combining with their results on the quark polarization,

$$\Delta u + \Delta d = 0.60 \pm 0.02, \qquad \Delta u - \Delta d = 1.08 \pm 0.02, \quad (7)$$

they concluded that the net orbital angular momentum (OAM) of the quarks is very small or consistent with zero:

$$2L^{u+d} = 0.06 \pm 0.14. \quad (8)$$

An independent study of $B^{u+d}_{20}(0)$ and $B^{u-d}_{20}(0)$ is reported by the LHPC Collaboration [12–15]:

$$B^{u+d}_{20}(0) = -0.09 \pm 0.03, \qquad B^{u-d}_{20}(0) = 0.67 \pm 0.03. \quad (9)$$

Using their previous results for the quark momentum fractions as well as the quark longitudinal polarizations [16],

$$\Delta\Sigma = 0.682 \pm 0.018, \quad (10)$$

they also estimated the quark orbital angular momentum to get

$$L^u = -0.088 \pm 0.019, \qquad L^d = 0.036 \pm 0.013, \quad (11)$$

or

$$\begin{aligned} 2L^{u+d} &= -0.104 \pm 0.038, \\ 2L^{u-d} &= -0.248 \pm 0.038. \end{aligned} \quad (12)$$

Their conclusion at this stage was as follows. Both flavors separately give a rather small contribution of the order of 17% (7%) for u-quark (d-quark) to the nucleon spin, due to cancellation in quark momentum fraction, spin and B_{20} [15]. Adding further u and d contributions give a very small and negative total orbital angular momentum.

Comparing the results of the two groups, one notices several discrepancies. For instance, the central value of the QCDSF prediction for $B^{u+d}_{20}(0)$ is small and positive, while the corresponding prediction by the LHPC group is small and negative. In spite of these discrepancies, a main conclusion of the two analyses was common: the net OAM carried by the quarks is very small or consistent with zero. As admitted by themselves, however, a main problem of their analyses was that these conclusions were obtained from the simulations performed with fairly large pion mass, ranging from 640 MeV to 1070 MeV.

Very recently, both groups carried out more refined analyses of the nucleon spin contents. The simulations were extended to much lower pion mass, and the results were further extrapolated to the physical pion mass with the help of chiral perturbation theory. We first review the main results of the LHPC Collaboration [17]. For the chiral extrapolation, they tried several versions of chiral perturbation theory, i.e., covariant baryon chiral perturbation theory (BChPT) and heavy baryon chiral perturbation theory (HBChPT) with and without the Δ resonance. The results obtained with the use of covariant BChPT are

$$A_{20}^{u+d}(0) = 0.520 \pm 0.014, \qquad A_{20}^{u-d}(0) = 0.157 \pm 0.006, \tag{13}$$

$$\begin{aligned} B_{20}^{u+d}(0) &= -0.094 \pm 0.050, \\ B_{20}^{u-d}(0) &= 0.274 \pm 0.037, \end{aligned} \tag{14}$$

which give

$$\begin{aligned} 2J^{u+d} &= 0.426 \pm 0.052, \\ 2J^{u} &= 0.428 \pm 0.032, \\ 2J^{d} &= -0.002 \pm 0.032. \end{aligned} \tag{15}$$

On the other hand, the predictions obtained with the HBChPT without the Δ resonance are given only for the isoscalar quantities:

$$A_{20}^{u+d}(0) = 0.485 \pm 0.014, \tag{16}$$

$$B_{20}^{u+d}(0) = 0.050 \pm 0.049, \tag{17}$$

which give

$$2J^{u+d} = 0.526 \pm 0.048. \tag{18}$$

One sees that the final answers are fairly sensitive to the ways of chiral extrapolation. In particular, $B_{20}^{u+d}(0)$, one of our central interests, is slightly negative in the covariant BChPT, while it is slightly positive in HBChPT. In either case, combined with their new preliminary estimate for the quark spin $\tilde{A}_{10}^{u+d}(t=0) = \Delta\Sigma^{u+d}$, they reconfirmed their previous conclusion that the net quark orbital angular momentum is nearly zero.

The QCDSF-UKQCD Collaboration also carried out a similar analysis [18]. Their main results are summarized as

$$A_{20}^{u+d}(0) = 0.572 \pm 0.012, \qquad A_{20}^{u-d}(0) = 0.198 \pm 0.008, \tag{19}$$

$$\begin{aligned} B_{20}^{u+d}(0) &= -0.120 \pm 0.023, \\ B_{20}^{u-d}(0) &= 0.269 \pm 0.020. \end{aligned} \tag{20}$$

We point out that these new results by the QCDSF-UKQCD group changed considerably from the previous QCDSF predictions obtained in the heavy-pion region several years ago [10,11]. This would mainly be an effect of chiral extrapolation to the physical pion mass. Putting aside moderate changes of $A_{20}^{u+d}(0)$ and $A_{20}^{u-d}(0)$, the changes of $B_{20}^{u+d}(0)$ and $B_{20}^{u-d}(0)$ are drastic. First, even the sign is changed for $B_{20}^{u+d}(0)$, although the fact, that its absolute value is relatively small, is intact. Also drastic is a considerable (more than a factor of 2) reduction of the magnitude of isovector $B_{20}^{u-d}(0)$. (This is also the case for the old and new LHPC predictions for $B_{20}^{u-d}(0)$ [14,15,17].) Here, we emphasize that this reduction was predicted in our theoretical analysis of $B_{20}^{u-d}(0)$ within the chiral quark soliton model [27]. In fact, it was shown there that this quantity has a strong pion mass dependence and that the lattice QCD predictions obtained in the heavy-pion region have a danger of overestimating it. The QCDSF-UKQCD Collaboration also carried out a new estimate of $\tilde{A}_{10}^{u+d}(0) = \Delta\Sigma^{u+d}$ [18] and obtained

$$\Delta\Sigma^{u+d} = 0.402 \pm 0.048. \tag{21}$$

Combining these, they finally obtain an estimate:

$$2J^{u+d} = 0.452 \pm 0.026, \qquad 2L^{u+d} = 0.050 \pm 0.054. \tag{22}$$

Thus, despite some appreciable changes of the predictions for some generalized form factors, a common conclusion of the two lattice QCD groups, that the net quark OAM is small, appears to be reconfirmed also by these new analyses.

Now we have a dilemma. Neither the intrinsic quark spin, the gluon polarization, nor the quark OAM seems to carry an adequate amount of angular momentum to saturate the total nucleon spin. Does it mean that the rest of the nucleon spin is mostly carried by the gluon OAM? As already mentioned, however, very large gluon OAM seems to contradict the recent claim by Brodsky and Gardner based on the observed small single-spin asymmetry on the deuteron target by the COMPASS group [21,22]. In our opinion, this confused status arises because we have not paid enough care to the fact that the decomposition of the nucleon spin is a highly scale-dependent idea. Later, we shall carry out an analysis, which pays more careful attention to the scale dependencies of the nucleon spin decomposition.

III. CHIRAL QUARK SOLITON MODEL PREDICTIONS

In a previous paper [27], we investigated the generalized form factors of the nucleon within the framework of the CQSM. A particular emphasis was put there on the pion mass dependence of the relevant quantities. (A similar analysis was carried out also in [28–30]. See also [31], in which the strong pion mass dependence of the net quark polarization $\Delta\Sigma$ in the chiral region was pointed out.) We discuss here only the predictions on $A_{20}^{u+d}(0)$, $B_{20}^{u+d}(0)$, $A_{20}^{u+d}(0)$, and $B_{20}^{u-d}(0)$, which provide us with enough information for the nucleon spin decomposition.

The largest discrepancy between the predictions of the CQSM and those of the lattice QCD simulations was observed for the isovector AGM $B_{20}^{u-d}(0)$ of the nucleon [27], so that we will start our discussion with this quantity. Within the framework of the CQSM, or more generally in any other low-energy models, the forward ($t \to 0$) limits of the isovector Pauli form factor $B_{10}^{u-d}(t)$ as well as the AGM form factor $B_{20}^{u-d}(t)$ are calculated as the difference of the standard and generalized Sachs magnetic and electric form factors at $t = 0$ as (see [27] for more details):

$$B_{10}^{u-d}(0) = G_{M,10}^{(I=1)}(0) - G_{E,10}^{(I=1)}(0), \tag{23}$$

$$B_{20}^{u-d}(0) = G_{M,20}^{(I=1)}(0) - G_{E,20}^{(I=1)}(0). \tag{24}$$

For completeness, we list below the theoretical expressions for the above quantities within the CQSM. The isovector electric form factor in the forward limit, i.e. $G_{E,10}^{(I=1)}(0)$, is just reduced to the isovector charge of the nucleon, which denotes that

$$G_{E,10}^{(I=1)}(0) = 1. \tag{25}$$

On the other hand, the isovector gravitomagnetic moment $G_{E,20}^{(I=1)}(0)$ is given as

$$G_{E,20}^{(I=1)}(0) = \frac{1}{M_N}\frac{1}{3I}\left(\frac{N_c}{2}\right)\sum_{m>0,n\le 0}\frac{1}{E_m - E_n}\langle m\|\boldsymbol{\tau}\|n\rangle \times\left\{\frac{E_m + E_n}{2}\langle m\|\boldsymbol{\tau}\|n\rangle + \langle m\|\frac{1}{3}(\boldsymbol{\alpha}\cdot\boldsymbol{p})\boldsymbol{\tau}\|n\rangle\right\}, \tag{26}$$

with M_N being the nucleon mass. Here, $|n\rangle$ and E_n are the eigenstates and the corresponding eigenenergies of the static Dirac Hamiltonian H with the hedgehog mean field, i.e.,

$$H|n\rangle = E_n|n\rangle, \tag{27}$$

where

$$H = \frac{\boldsymbol{\alpha}\cdot\nabla}{i} + \beta M[\cos F(r) + i\gamma_5\boldsymbol{\tau}\cdot\hat{\boldsymbol{r}}\sin F(r)], \tag{28}$$

with M being the dynamical quark mass. The symbols $\sum_{n\le 0}$ and $\sum_{m>0}$ stand for the summation over all the occupied and unoccupied single-quark eigenstates of H. (The fact that $G_{E,20}^{(I=1)}(0)$ is given as a double sum over the single-quark orbitals is connected with the fact that it vanishes at the mean-field level and survives only at the first order in the collective angular velocity of the soliton.)

Concerning the isovector magnetic moment $G_{M,10}^{(I=1)}(0)$ and the corresponding isovector gravitomagnetic moment $G_{M,20}^{(I=1)}(0)$, some comments are in order. In our previous study [27], we have calculated only the leading-order contributions to these quantities and neglected the subleading $1/N_c$ corrections, for simplicity. In the present study, we shall include the latter as well. The reason is because a similar $1/N_c$ correction (or more concretely, the first-order rotational correction in the collective angular velocity of the soliton) is known to be important for resolving the famous underestimation problem of some isovector observables, like the isovector axial-charge, inherent in the hedgehog-type soliton model [32–34]. Taking account of this first-order rotational correction, the isovector magnetic moment of the nucleon consists of the leading $O(\Omega^0)$ term and the subleading $O(\Omega^1)$ term as

$$G_{M,10}^{(I=1)}(0) = G_{M,10}^{(I=1)\Omega^0}(0) + G_{M,10}^{(I=1)\Omega^1}(0), \tag{29}$$

where

$$G_{M,10}^{(I=1)\Omega^0}(0) = -\frac{M_N}{9}N_c\sum_{n\le 0}\langle n\|(\boldsymbol{x}\times\boldsymbol{\alpha})\cdot\boldsymbol{\tau}\|n\rangle, \tag{30}$$

$$G_{M,10}^{(I=1)\Omega^1}(0) = -i\frac{M_N}{9I}\left(\frac{N_c}{2}\right)\sum_{m>0,n\le 0}\frac{1}{E_m - E_n}\langle m\|\boldsymbol{\tau}\|n\rangle \times\langle m\|(\boldsymbol{x}\times\boldsymbol{\alpha})\times\boldsymbol{\tau}\|n\rangle. \tag{31}$$

Similarly, $G_{M,20}^{(I=1)}(0)$ is given as a sum of the $O(\Omega^0)$ and the $O(\Omega^1)$ terms:

$$G_{M,20}^{(I=1)}(0) = G_{M,20}^{(I=1)\Omega^0}(0) + G_{M,20}^{(I=1)\Omega^1}(0), \tag{32}$$

where

$$G_{M,20}^{(I=1)\Omega^0}(0) = -\frac{1}{9}N_c\sum_{n\le 0}\{E_n\langle n\|(\boldsymbol{x}\times\boldsymbol{\alpha})\cdot\boldsymbol{\tau}\|n\rangle + \langle n\|\boldsymbol{L}\cdot\boldsymbol{\tau}\|n\rangle\}, \tag{33}$$

$$G_{M,20}^{(I=1)\Omega^1}(0) = -i\frac{1}{9I}\left(\frac{N_c}{2}\right)\sum_{m>0,n\le 0}\frac{1}{E_m - E_n}\langle m\|\boldsymbol{\tau}\|n\rangle \times\left\{\frac{E_m + E_n}{2}\langle m\|(\boldsymbol{x}\times\boldsymbol{\alpha})\times\boldsymbol{\tau}\|n\rangle + \langle m\|\boldsymbol{L}\times\boldsymbol{\tau}\|n\rangle\right\}. \tag{34}$$

As usual, the above sums over the eigenstates of H can be evaluated with use of the discretized momentum basis of Kahana and Ripka [35,36]. (Some generalization of the Kahana-Ripka basis is necessary for the evaluation of the $O(\Omega^1)$ terms including double sums [37].) Now, we are ready to show the results of our numerical calculation. Similarly to the analysis reported in [27], we see the effect of varying the pion mass m_π, by fixing the dynamical quark mass M to be 400 MeV. For that purpose, we prepare self-consistent soliton solutions for seven values of m_π, i.e., $m_\pi = 0$, 100, 200, 300, 400, 500, and 600 MeV, within the double-subtraction Pauli-Villars regularization scheme [38]. Favorable physical predictions will be obtained by using the value $M = 400$ MeV and $m_\pi = 100$ MeV, since this set gives a self-consistent solution close to the phenomenologically successful one obtained with $M = 375$ MeV and $m_\pi = 0$ MeV in the single-subtraction Pauli-Villars regularization scheme [39–41]. (For the nucleon mass M_N, appearing in the above formulas of the generalized form factors, the theoretical consistency requires us to use self-consistent soliton masses. Otherwise, fundamental conservation laws like the momentum sum rule would be violated. See [27] for the details.)

Table I shows the theoretical predictions for the isovector magnetic moment of the nucleon, in dependence of the pion mass m_π. The second and the third columns, respec-

TABLE I. The CQSM predictions for the isovector magnetic moment of the nucleon in dependence of the pion mass. See the text for more detailed explanation.

m_π (MeV)	$G_{M,10}^{(I=1)\Omega^0}(0)$	$G_{M,10}^{(I=1)\Omega^1}(0)$	$G_{M,10}^{(I=1)\Omega^0+\Omega^1}(0)$
0	4.12	1.14	5.26
100	3.41	1.24	4.64
200	2.89	1.39	4.28
300	2.69	1.53	4.21
400	2.67	1.66	4.33
500	2.72	1.80	4.52
600	2.73	1.99	4.72

tively, stand for the $O(\Omega^0)$ and the $O(\Omega^1)$ contributions, while their sums are shown in the fourth column. One can be convinced that the first-order rotational correction is very important for these isovector observables. With the favorable set of parameters, i.e., $m_\pi = 100$ MeV with $M = 400$ MeV, the theory gives $\mu_p - \mu_n = G_{M,10}^{(I=1)}(0) \simeq 4.64$, which is remarkably close to the empirically known isovector magnetic moment of the nucleon:

$$(\mu_p - \mu_n)^{\rm exp} = 4.70589. \tag{35}$$

Next, shown in Table II are the predictions of the CQSM for relevant generalized form factors in the forward limit, as functions of m_π, which are necessary to evaluate the isovector AGM. The second and the third columns of this table, respectively, stand for the isovector gravitomagnetic moment and the gravitoelectric moment, while the fourth column represents the leading-order contribution to the isovector AGM of the nucleon. Note that the numbers in the fourth column are obtained as the difference of those in the second and the third columns, according to the formula, $B_{M,20}^{(u-d)\Omega^0}(0) \equiv G_{M,20}^{(I=1)}(0) - G_{E,20}^{(I=1)}(0)$. These are the predictions already given in our previous paper. What is new here is the fifth column, which represents the first-order rotational correction to the isovector AGM of the nucleon. We have already seen that the first-order rotational correction is very important for reproducing the observed isovector magnetic moment of the nucleon. Table II shows that the effect of the first-order rotational correction is even more drastic for the isovector AGM of the nucleon. This is because the leading-order estimate of the isovector AGM shown in the third column is obtained as the difference of the two quantities $G_{M,20}^{(I=1)}(0)$ and $G_{E,20}^{(I=1)}(0)$, having the same size of magnitude, and a sizable cancellation occurs between them. As a consequence, the final predictions of the CQSM for the isovector AGM of the nucleon, given in the seventh column are nearly a factor of 3 or 4 larger than our previous results neglecting the first-order rotational correction.

At this stage, one might be interested in a comparison with the predictions of lattice QCD. One must be careful here. Different from the anomalous magnetic moment of the nucleon, which is scale independent due to the conservation of the electromagnetic current, the anomalous gravitomagnetic moment is a scale-dependent quantity. The predictions of the lattice QCD simulations correspond to the renormalization scale of $Q^2 \simeq 4$ GeV^2, while the predictions of the CQSM are thought to correspond to a much lower energy scale around $Q^2 = 0.30$ GeV^2. Fortunately, by making use of Ji's observation that J^q and $\langle x \rangle^q$ obey exactly the same evolution equation, we can figure out the scale dependence of $B_{20}^{u-d}(0)$. (See the next section, for more details.) From the predictions of the CQSM for $B_{20}^{u-d}(0)$ given in the sixth column, we have estimated the corresponding values at $Q^2 = 4$ GeV^2. The results are shown in the seventh column of Table II. For the favorable pion mass parameter $m_\pi = 100$ MeV, our estimate gives $B_{20}^{u=d}(0) \simeq 0.289$, which should be compared with the corresponding prediction $B_{20}^{u-d}(0) = 0.274 \pm 0.037$ of the new LHPC lattice simulation [17], and $B_{20}^{u-d}(0) = 0.269 \pm 0.020$ of the QCDSF-UKQCD one [18]. One finds that the predictions of the CQSM and those of the lattice QCD simulations are now remarkably close to each other. This is a welcome result, since it is thought to give strong support to the reliability of the theoretical predictions on the isovector AGM of the nucleon $B_{20}^{u-d}(0)$.

After obtaining a refined estimate of $B_{20}^{u-d}(0)$ within the framework of the CQSM, we revise Fig. 5b in our previous paper [27]. The filled circles in Fig. 1 are the CQSM predictions of $B_{20}^{u-d}(0)$ corresponding to the scale $Q^2 = 4$ GeV^2, in dependence of the pion mass. The corresponding predictions of the QCDSF and LHPC Collaborations carried out in the heavy-pion region several years ago are

TABLE II. The CQSM predictions for the isovector AGM of the nucleon in dependence of the pion mass. See the text for more detailed explanation.

m_π (MeV)	$G_{M,20}^{(I=1)}(0)$	$G_{E,20}^{(I=1)}(0)$	$B_{20}^{(u-d)\Omega^0}(0)$	$B_{20}^{(u-d)\Omega^1}(0)$	$B_{20}^{u-d}(0)$	$B_{20}^{u-d}(0)$ at $Q^2 = 4$ GeV^2
0	0.361	0.228	0.133	0.272	0.405	0.256
100	0.392	0.276	0.116	0.342	0.458	0.289
200	0.452	0.327	0.125	0.429	0.554	0.350
300	0.519	0.350	0.169	0.491	0.660	0.418
400	0.579	0.354	0.225	0.534	0.759	0.480
500	0.640	0.347	0.293	0.567	0.860	0.544
600	0.716	0.328	0.388	0.600	0.988	0.625

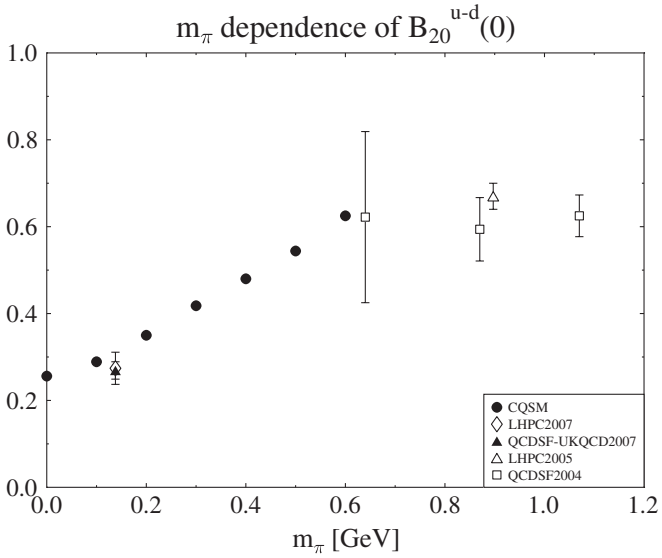

FIG. 1. The pion mass dependence of $B_{20}^{u-d}(0)$ predicted by the CQSM, in comparison with the old and new lattice QCD predictions. Both correspond to the scale $Q^2 \simeq 4$ GeV^2.

represented by the open squares and the open triangles [10,15]. On the other hand, the new predictions by the LHPC and QCDSF-UKQCD Collaborations, extrapolated to the physical pion mass by utilizing the chiral perturbation theory, are shown, respectively, by the open diamond and the filled triangles [17,18]. One sees that the effect of chiral extrapolation is drastic such that the new predictions of the lattice QCD are more than a factor of 2 smaller than the old predictions given in the heavy-pion region. This sizable reduction is just consistent with our analysis based on the CQSM [27]. Now, one can be convinced that the predictions of the CQSM and the lattice QCD for the isovector AGM of the nucleon $B_{20}^{u-d}(0)$ are mutually consistent.

Next, we turn to the discussion of more difficult isoscalar quantities. As shown in [27,28], the CQSM predicts that

$$A_{20}^{u+d}(0) = \langle x \rangle^{u+d} = 1, \qquad B_{20}^{u+d}(0) = 0. \tag{36}$$

It should be noticed that these equalities hold irrespective of the pion mass within the model. The first relation is only natural. It simply means that the momentum sum rule is saturated by the quark fields alone in this effective quark model, which does not contain explicit gluon degrees of freedom. The second relation holds by the similar reason. From Ji's angular momentum sum rule, we generally have (in the two flavor case)

$$2(J^{u+d} + J^g) = \langle x \rangle^{u+d} + B_{20}^{u+d}(0) + \langle x \rangle^g + B_{20}^g(0) = 1. \tag{37}$$

If this is combined with the momentum sum rule of QCD,

$$\langle x \rangle^{u+d} + \langle x \rangle^g = 1, \tag{38}$$

we are led to a novel identity,

$$B_{20}^{u+d}(0) + B_{20}^g(0) = 0, \tag{39}$$

which dictates that the total nucleon AGM (quark plus gluon contributions) vanishes identically. The answer $B_{20}^{u+d}(0) = 0$ is therefore an inevitable conclusion of any effective quark model without gluon fields. In both of the LHPC and QCDSF lattice QCD simulations carried out in the heavy-pion region several years ago, the magnitude of $B_{20}^{u+d}(0)$ was found to be fairly small [11,12]. Since $B_{20}^{u+d}(0)$ is equal to the difference of $2J^{u+d}$ and $\langle x \rangle^{u+d}$, the small values of the lattice QCD predictions for $B_{20}^{u+d}(0)$ at this point were interpreted to indicate approximate equality of the total angular momentum and linear momentum fractions of quarks and gluons as advocated by Teryaev several years ago [42,43]. However, the recently performed ChPT fits by the LHPC and QCDSF-UKQCD Collaborations appear to indicate a sizable bending through the chiral extrapolation in the low pion mass region, leading to negative $B_{20}^{u+d}(0)$ of the order of -0.1, although one must be very careful about the fact that the final conclusion depends on the ways of the chiral extrapolation method [17,18].

Under such circumstances, it would be fine if we can give some useful constraint on the magnitude of $B_{20}^{u+d}(0)$. To this end, we first recall the fact that $B_{20}^{u+d}(0)$ is given as the second moment of the forward limit of the unpolarized spin-flip GPD $E^{u+d}(x, \xi, t)$ as

$$B_{20}^{u+d}(0) = \int_{-1}^{1} x E^{u+d}(x, 0, 0) dx. \tag{40}$$

It is important to recognize that the first moment of the same quantity gives the isoscalar magnetic moment of the nucleon up to a factor of 3:

$$B_{10}^{u+d}(0) = \int_{-1}^{1} E^{u+d}(x, 0, 0) dx = \kappa^{u+d} = 3(\kappa^p + \kappa^n). \tag{41}$$

The forward limit of the GPD $E^{u+d}(x, 0, 0)$ was calculated within the framework of the CQSM by Ossmann *et al.* [44]. (There is also a calculation for the forward limit of the isovector GPD $E^{u-d}(x, 0, 0)$ within the CQSM [45].) It is given as a sum of the two part, i.e., the contribution of $N_c(= 3)$ valence quarks and that of the vacuum-polarized Dirac-sea quarks as

$$E^{u+d}(x, 0, 0) = E_{val}^{u+d}(x, 0, 0) + E_{v.p.}^{u+d}(x, 0, 0). \tag{42}$$

There are interesting findings that the valence quark term turns out to have a similar shape as the corresponding valence term $f_{val}^{u+d}(x)$ of the standard unpolarized PDF, while the deformed Dirac-sea contribution has a strong chiral enhancement near $x = 0$, which is antisymmetric with respect to the transformation $x \rightarrow -x$. (Note that the antisymmetric nature of the Dirac-sea contribution to $E^{u+d}(x, 0, 0)$ means that it gives no contribution to its first moment.) Following the schematic analysis carried out in

[46] (see also [27]), we therefore propose to parametrize the characteristic feature of $E^{u+d}(x,0,0)$ in the following simple form:

$$E^{u+d}(x,0,0) = Cf_{val}^{u+d}(x) - D\delta'(x), \tag{43}$$

with $C<0$ and $D>0$. With this schematic parametrization, the first and the second moment sum rules of $E^{u+d}(x,0,0)$ become

$$\int_{-1}^{1} E^{u+d}(x,0,0)dx = 3C = 3(\kappa^p + \kappa^n), \tag{44}$$

$$\int_{-1}^{1} xE^{u+d}(x,0,0)dx = C\int_{-1}^{1} f_{val}^{u+d}(x)dx + D. \tag{45}$$

Using the observed anomalous magnetic moments of the proton and the neutron, the first relation gives

$$C = (\kappa^p + \kappa^n)^{\rm exp} = -0.120. \tag{46}$$

On the other hand, the second relation gives

$$B_{20}^{u+d}(0) = C\int_{-1}^{1} f_{val}^{u+d}(x)dx + D. \tag{47}$$

As a matter of course, in the CQSM, the valence and the vacuum polarization contributions in (47) exactly cancel each other so that the identity $B_{20}^{u+d}(0)=0$ holds. Such an exact cancellation may not happen in real QCD, which contains the gluon fields as well. Nonetheless, it is reasonable to expect that the general shape of $E^{u+d}(x,0,0)$ predicted by the CQSM, especially its chiral behavior observed in the small x region, would be preserved when going to real QCD, which in turn strongly indicates that there will be no change of sign in the contribution of the sea-quark-like component to $B_{20}^{u+d}(0)$. We thus conjecture that the coefficient D in (47) is at least larger than or equal to 0. Combining this with the fact that $\int_{-1}^{1} f_{\rm val}^{u+d}(x)$ is smaller than 1 (this is because the sea-quark-like component also carries some portion of the total momentum fraction of the nucleon), we would then conclude from (47) that the lower limit of $B_{20}^{u+d}(0)$ is $-0.12(=(\kappa^p+\kappa^n)^{\rm exp})$. In carrying out a semiempirical analysis of the nucleon spin contents in the next section, we therefore take a standpoint that the precise value of $B_{20}^{u+d}(0)$ is still uncertain, but it lies most likely in the range

$$-0.12 \le B_{20}^{u+d}(0) \le 0. \tag{48}$$

This is the main theoretical uncertainty in our semiphenomenological analysis of the nucleon spin contents carried out in the next section.

IV. SEMI-EMPIRICAL ESTIMATE OF NUCLEON SPIN CONTENTS

Now, we are ready to start our semiempirical analysis of the nucleon spin contents. Our strategy here is to use empirical information as much as possible, if available. To explain our approach more concretely, we start again with Ji's angular momentum sum rule written in a slightly more general form:

$$\frac{1}{2} = J^Q + J^g, \tag{49}$$

with

$$J^Q = \frac{1}{2}[\langle x\rangle^Q + B_{20}^Q(0)], \qquad J^g = \frac{1}{2}[\langle x\rangle^g + B_{20}^g(0)]. \tag{50}$$

Here, Q denotes the sum of all active quark flavors. ($Q=u+d$ for the two-flavor case, and $Q=u+d+s$ for the three-flavor case.) To carry out flavor decomposition of the total quark angular momentum, we also need another combination of Ji's sum rule:

$$J^{u-d} = \frac{1}{2}[\langle x\rangle^{u-d} + B_{20}^{u-d}(0)]. \tag{51}$$

We emphasize again that the momentum fractions $\langle x\rangle^Q$, $\langle x\rangle^{u-d}$, and $\langle x\rangle^g$ are all empirically well determined. Naturally, these momentum fractions are all scale-dependent quantities. A key observation here, first made by Ji [23,26], is that J^Q and J^g obey exactly the same evolution equations as $\langle x\rangle^Q$ and $\langle x\rangle^g$ do. According to him, the underlying reason is that forming spatial moment of energy momentum operator does not change short-distance singularity of the operator. The solution of this (coupled) evolution equation is extremely simple at the leading order (LO):

$$2J^Q(Q^2) = \frac{3n_f}{16+3n_f} + \left(\frac{\ln Q_0^2/\Lambda^2}{\ln Q^2/\Lambda^2}\right)^{2(16+3n_f)/(33-2n_f)} \times\left[2J^Q(Q_0^2) - \frac{3n_f}{16+3n_f}\right], \tag{52}$$

$$2J^g(Q^2) = \frac{16}{16+3n_f} + \left(\frac{\ln Q_0^2/\Lambda^2}{\ln Q^2/\Lambda^2}\right)^{2(16+3n_f)/(33-2n_f)} \times\left[2J^g(Q_0^2) - \frac{16}{16+3n_f}\right]. \tag{53}$$

Particularly interesting here are the asymptotic values in the $Q^2\to\infty$ limit:

$$2J^Q(\infty) = \frac{3n_f}{16+3n_f}, \qquad 2J^g(\infty) = \frac{16}{16+3n_f}. \tag{54}$$

Numerically, we obtain

$$2J^Q(\infty) \simeq 0.529, \qquad 2J^g(\infty) \simeq 0.471, \tag{55}$$

for $n_f=6$, while

$$2J^Q(\infty) \simeq 0.360, \qquad 2J^g(\infty) \simeq 0.640, \tag{56}$$

for $n_f=3$.

In our actual analysis below, we take account of the scale dependencies of the relevant quantities by using the known

evolution equations at the next-to-leading order (NLO) for the momentum fractions, making full use of the fact that J^q and $\langle x\rangle^q$ (and also J^g and $\langle x\rangle^g$) obey the same evolution equations. For the sake of completeness, we write down here the relevant NLO equations, which we use in the following analysis. The singlet moments J^Q and J^g (and also $\langle x\rangle^Q$ and $\langle x\rangle^g$) evolve as (see, for example, [47–49])

$$\begin{pmatrix} J^Q(Q^2) \\ J^g(Q^2) \end{pmatrix} = \left\{ \left(\frac{\alpha_S(Q^2)}{\alpha_S(Q_0^2)} \right)^{\lambda_-/2\beta_0} \left[\boldsymbol{P}_- - \frac{1}{2\beta_0} \times \frac{\alpha_S(Q_0^2) - \alpha_S(Q^2)}{4\pi} \boldsymbol{P}_- \boldsymbol{R} \boldsymbol{P}_- - \left(\frac{\alpha_S(Q_0^2)}{4\pi} - \frac{\alpha_S(Q^2)}{4\pi} \left(\frac{\alpha_S(Q^2)}{\alpha_S(Q_0^2)} \right)^{(\lambda_+ - \lambda_-)/2\beta_0} \right) \times \frac{\boldsymbol{P}_- \boldsymbol{R} \boldsymbol{P}_+}{2\beta_0 + \lambda_+ - \lambda_-} \right] + (+ \leftrightarrow -) \right\} \begin{pmatrix} J^Q(Q_0^2) \\ J^g(Q_0^2) \end{pmatrix}. \tag{57}$$

Here, $\alpha_S(Q^2)$ is the QCD running coupling constant at the NLO given by

$$\alpha_S(Q^2) = \frac{4\pi}{\beta_0 \ln(Q^2/\Lambda^2)} \left[1 - \frac{\beta_1 \ln\ln(Q^2/\Lambda^2)}{\beta_0^2 \ln(Q^2/\Lambda^2)} \right], \tag{58}$$

with the choice $\Lambda = 0.248$ GeV, while $\beta_0 = 11 - \frac{2}{3} n_f$ and $\beta_1 = 102 - \frac{38}{3} n_f$ with n_f being the active number of quark flavor. The quantities $\boldsymbol{R}$ and $\boldsymbol{P}_\pm$ are defined by

$$\boldsymbol{R} = \boldsymbol{\gamma}^{(1)} - \frac{\beta_1}{\beta_0} \boldsymbol{\gamma}^{(0)}, \tag{59}$$

$$\boldsymbol{P}_\pm = \pm \frac{\boldsymbol{\gamma}^{(0)} - \lambda_\mp}{\lambda_+ - \lambda_-}, \tag{60}$$

where $\boldsymbol{\gamma}^{(0)}$ and $\boldsymbol{\gamma}^{(1)}$ are the relevant anomalous dimension matrices at the LO and NLO, respectively, given by [50–52]

$$\boldsymbol{\gamma}^{(0)} = \begin{pmatrix} 64/9 & -4n_f/3 \\ -64/9 & 4n_f/3 \end{pmatrix} \tag{61}$$

and

$$\boldsymbol{\gamma}^{(1)} = \frac{64}{243} \begin{pmatrix} 367 - 39n_f & -\frac{1833}{32} n_f \\ -(367 - 39n_f) & \frac{1833}{32} n_f \end{pmatrix} \tag{62}$$

while $\lambda_\pm$ are the two eigenvalues of the LO anomalous dimension matrix $\boldsymbol{\gamma}^{(0)}$.

On the other hand, the nonsinglet (NS) moments evolve as [47–49]

$$J_{\rm NS}(Q^2) = \left[1 + \frac{\alpha_S(Q^2) - \alpha_S(Q_0^2)}{4\pi} \left(\frac{\gamma_{\rm NS}^{(1)}}{2\beta_0} - \frac{\beta_1 \gamma_{\rm NS}^{(0)}}{2\beta_0^2} \right) \right] \times \left(\frac{\alpha_S(Q^2)}{\alpha_S(Q_0^2)} \right)^{\gamma_{\rm NS}^{(0)}/2\beta_0} J_{\rm NS}(Q_0^2), \tag{63}$$

with

$$\gamma_{\rm NS}^{(0)} = \frac{64}{9}, \qquad \gamma_{\rm NS}^{(1)} = \frac{64}{243}(367 - 39n_f). \tag{64}$$

Here, it is understood that, for $n_f = 3$, $J_{\rm NS}$ stands for either $J^{(3)} \equiv J^u - J^d$ or $J^{(8)} \equiv J^u + J^d - 2J^s$.

Now, we are left with two quantities, $B_{20}^{u+d}(0)$ and $B_{20}^{u-d}(0)$, which are yet empirically unknown. Here, one might be tempted to use lattice QCD predictions for those. In our opinion, however, blind acceptance of the lattice QCD predictions at the present stage is a little dangerous, especially because there seems to be large uncertainties in the process of chiral extrapolation. We proceed slightly more cautiously by also taking account of the information from a phenomenologically successful low-energy model of the nucleon, i.e., the CQSM.

After explaining our general strategy, let us now start our semiphenomenological analysis of the nucleon spin contents. We start with the empirical information obtained from the MRST2004 as well as the CTEQ5 fits [53,54]. As already emphasized, these two popular PDF fits give almost the same quark and gluon momentum fractions below the energy scale $Q^2 \simeq 10$ GeV^2, Although these PFDs are given basically above $Q^2 \simeq 1$ GeV^2, we try to see what happens if we evolve down these fits to a lower energy scale as $Q^2 \simeq 0.30$ GeV$^2 \simeq (600$ MeV$)^2$, which is understood to be the energy scale of the CQSM. Using the known NLO evolution equations for $\langle x\rangle^Q$ and $\langle x\rangle^g$, together with the MRST2004 predictions [53],

$$\langle x\rangle^Q \simeq 0.578, \qquad \langle x\rangle^g \simeq 0.422 \quad \text{at } Q^2 = 4 \text{ GeV}^2, \tag{65}$$

we have estimated the scale dependencies of $\langle x\rangle^Q$ and $\langle x\rangle^g$ in the range 0.30 GeV$^2 \le Q^2 \le 4$ GeV^2. The result is shown in Fig. 2. One sees that the scale dependencies of the quark and gluon momentum fractions are fairly strong below $Q^2 \simeq 1$ GeV^2. At the low-energy scale around $Q^2 \simeq 0.30$ GeV^2, one finds that the momentum fraction carried by the quarks is nearly 80%, while that of the gluons is about 20%.

As a matter of course, the standard view is that the applicability range of the perturbative QCD is at least above 1 GeV, so that one might be a little suspicious of the physical significance of such "disevolution" to low-energy scales. Still, we believe it is meaningful for the following reason. Basically, we are following the spirit of PDF fits by Glück, Reya, and Vogt [47,48]. As is well known, these authors start the QCD evolution at the exceptionally low-energy scales, i.e., $Q_{\rm ini}^2 \simeq 0.23$ GeV^2 in the leading-order case, and $Q_{\rm ini}^2 \simeq 0.34$ GeV^2 in the NLO case. They thus found that, even at such low-energy scales, they absolutely need nonperturbatively (or dynamically) generated sea-quarks, which may be interpreted as the effects of meson clouds. We believe such analyses (somewhat nonstandard from the viewpoint of more conservative use of the perturbative QCD) play an important role to connect

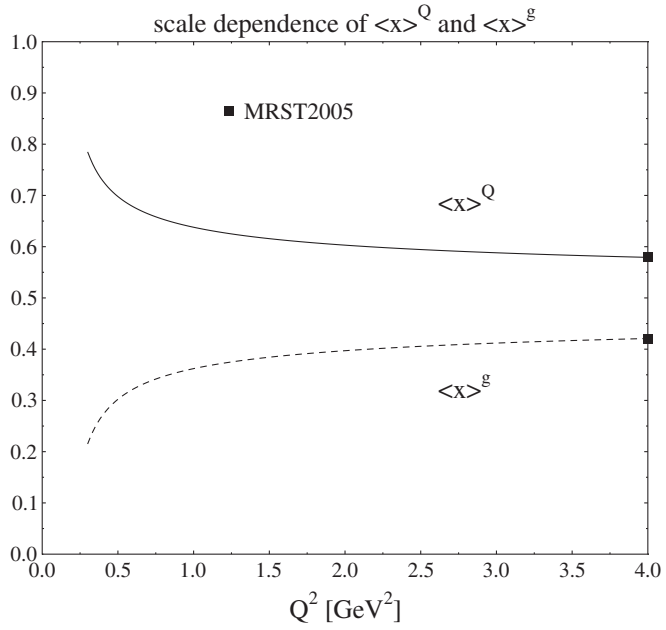

FIG. 2. The scale dependencies of the quark and gluon momentum fractions, which reproduce the MRST fits at $Q^2 = 4$ GeV^2.

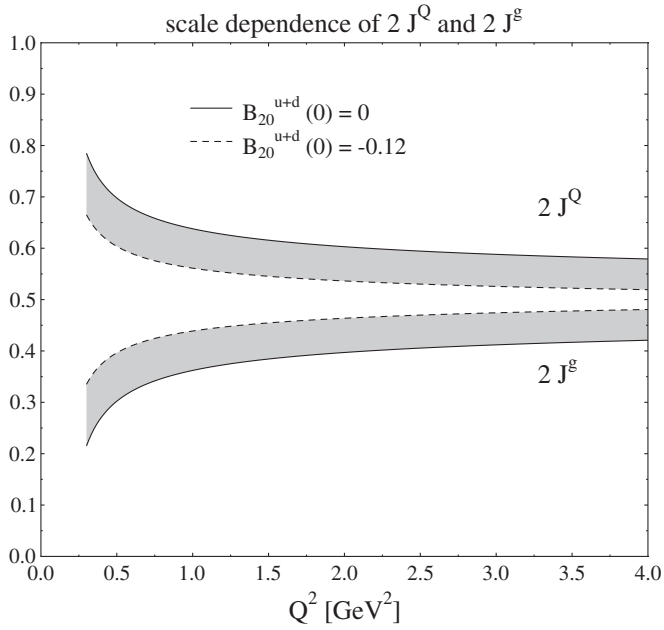

FIG. 3. The scale dependencies of the quark and gluon angular momentum fractions. The solid and dashed curves, respectively, correspond to the choices $B_{20}^{u+d}(0) = 0$ and $B_{20}^{u+d}(0) = -0.12$.

the physics of nonperturbative QCD in the low-energy domain and the perturbative QCD in the high-energy deep-inelastic-scattering (DIS) domain. In fact, we have carried out several theoretical analyses based on the GRV spirit. That is, we use the predictions of the CQSM for various PDFs as initial-scale distributions given at the low-energy scale around 600 MeV. After evolving them with use of the NLO evolution equation, we compare the resultant predictions with the corresponding DIS observables with a remarkable success without any other adjustable parameters [39,40,55–58]. Then, we shall continue our analysis by accepting the viewpoint that the energy scale between 600 MeV and 1 GeV is an important region, which connects the low-energy nonperturbative physics and the high-energy perturbative physics of QCD.

Now, we show in Fig. 3 our estimate of the scale dependence of the total angular momentum fractions carried by the quarks and the gluons. They are obtained in the following way. As argued in [27], if the net quark contribution to the nucleon AGM vanishes, i.e., $B_{20}^{u+d}(0) = 0$, we have extremely simple proportionality relations as

$$J^Q = \frac{1}{2}\langle x\rangle^Q, \qquad J^g = \frac{1}{2}\langle x\rangle^g, \tag{66}$$

which was advocated by Teryaev based on the equivalence principle some years ago [42,43,59]. Very interestingly, these proportionality relations hold independent of the energy scale, since (J^Q, J^g) and $(\langle x\rangle^Q, \langle x\rangle^g)$ obey the same evolution equations. Thus, the solid curves in Fig. 3 are nothing different from the curves for $\langle x\rangle^Q$ and $\langle x\rangle^g$ in Fig. 2. On the other hand, the dashed curves correspond to another extreme, which is obtained by using the value $B_{20}^{u+d}(0) = -0.12$ at $Q^2 = 0.30$ GeV^2. With this negative value of $B_{20}^{u+d}(0)$, $2J^Q$ becomes a little smaller and $2J^g$ becomes a little larger as compared with the case $B_{20}^{u+d}(0) = 0$. Still, one notices that, at the scale $Q^2 \simeq 0.30$ GeV^2, the quarks carry about 65% of the total angular momentum fraction. At the moment, there is a sizable ambiguity in the magnitude of $B_{20}^{u+d}(0)$, but we believe that the truth lies between the two extreme cases illustrated in Fig. 3. (See the discussion at the end of the previous section.)

Now, the net orbital angular momentum fractions carried by the quarks can be obtained by subtracting $\Delta\Sigma$ from $2J^Q$. Since the prediction of the CQSM at $Q^2 \simeq 5$ GeV^2 is remarkably close to the central value $\Delta\Sigma = 0.33$ of the recent HERMES analysis, we use this HERMES value here. To make the discussion simple, we shall neglect here the scale dependence of $\Delta\Sigma$. (In the $\overline{\text{MS}}$ scheme at the NLO, $\Delta\Sigma$ is known to have a weak scale dependence due to the coupling with Δg. This scale dependence is very weak, however.)

Shown in Fig. 4 are $2L^Q$, $\Delta\Sigma$, and $2J^g$ as functions of Q^2. Here, the solid and dashed curves correspond to the cases $B_{20}^{u+d}(0) = 0$ and $B_{20}^{u+d}(0) = -0.12$, respectively. First, let us look into the case $B_{20}^{u+d}(0) = 0$. In this case, there is a crossover around $Q^2 \simeq 0.7$ GeV$^2 \simeq (840$ MeV$)^2$, where the magnitudes of $2L^Q$, $\Delta\Sigma$, and $2J^g$ are all approximately equal,

$$2L^Q \simeq \Delta\Sigma \simeq 2J^g \simeq 1/3. \tag{67}$$

One sees that L^Q is a rapidly decreasing function of Q^2, so

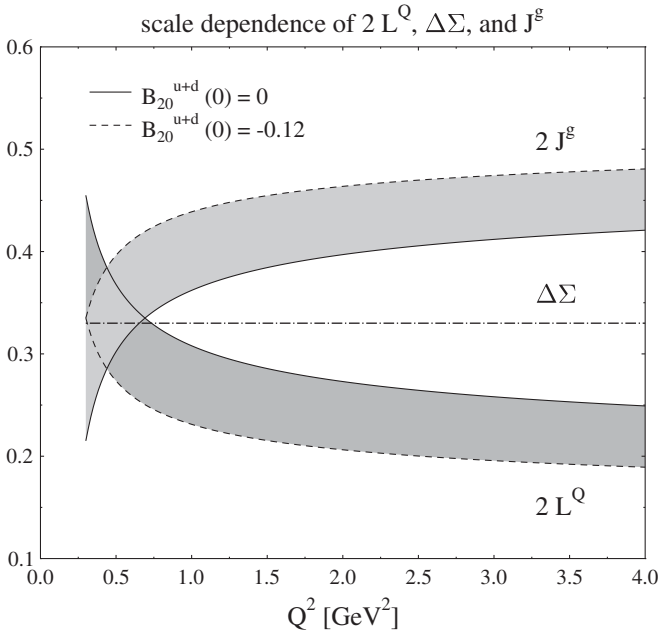

FIG. 4. The scale dependencies of the total angular momentum and orbital angular momentum of quarks, together with the net longitudinal polarization of quarks. The solid and dashed curves, respectively, correspond to the choices $B_{20}^{u+d}(0) = 0$ and $B_{20}^{u+d}(0) = -0.12$.

that, as Q^2 increases beyond this crossover energy scale, L^Q becomes less and less important as compared with $\Delta\Sigma$ and J^Q. However, the fact that L^Q is a rapidly decreasing function below 1 GeV conversely means that it must be very large at the low-energy scale around 600 MeV, which we emphasize is qualitatively consistent with the picture of the CQSM [37,60].

Next, we turn to the case $B_{20}^{u+d}(0) = -0.12$. In this case, the crossover, where $2L^Q \simeq \Delta\Sigma \simeq 2J^g \simeq 1/3$, occurs around the energy scale $Q^2 \simeq 0.30$ GeV^2. Although the role of quark OAM is less important as compared with the case corresponding to $B_{20}^{u+d}(0) = 0$, it still carries about $1/3$ of the total nucleon spin at this low-energy scale. We emphasize that this is an inevitable conclusion of believing the QCD evolution equation, since it tells us that, at this low-energy scale, the gluon (spin plus OAM) carries at most $1/3$ of the total nucleon spin, so that what remains to carry the remainder $1/3$ of the nucleon spin must be the quark OAM. On the other hand, when going to higher energy scale, say at $Q^2 \simeq 4$ GeV^2, corresponding to the renormalization scale of the lattice QCD calculations, one sees that the amount of the quark OAM becomes much smaller. Still, it is seen to carry nearly 20% of the total nucleon spin even at $Q^2 \simeq 4$ GeV^2. One might suspect that this would contradict the conclusion of the lattice QCD analyses. Probably, the main cause of discrepancy can be traced back to a little overestimation of the net quark polarization $\Delta\Sigma$ in the lattice QCD. In fact, the result of the QCDSF-UKQCD group for $\Delta\Sigma$ is 0.402 ± 0.024 [18], which overestimates a little the central value 0.33 of the HERMES analysis [9], which we have used in our semi-empirical analysis here. (One of the reasons of a little overestimation of $\Delta\Sigma$ in the lattice QCD simulations may be attributed to the so-called quenched approximation, i.e., the neglect of the disconnected diagrams.) In our opinion, the quark OAM fraction of the order of 20% is reasonable enough from the following simple consideration. To prove this statement, we recall that the asymptotic value (the value in the $Q^2 \to \infty$ limit) of the total angular momentum fractions of the quarks and the gluons is extracted from the relations (52) and (53), which follows from the fact that (J^Q, J^g) and $(\langle x\rangle^Q, \langle x\rangle^g)$ obey the same evolution equation. With the realistic case of six flavors, we have

$$2J^Q(\infty) \simeq 0.529, \qquad 2J^g(\infty) \simeq 0.471. \tag{68}$$

Subtracting $\Delta\Sigma \simeq 0.33$, which is thought to be nearly scale independent, we thus obtain

$$2L^Q(\infty) \simeq 0.199. \tag{69}$$

Since L^Q is a decreasing function of Q^2, the magnitude of $2L^Q$ at the scale $Q^2 \simeq 4$ GeV^2 must be larger or at least approximately equal to this asymptotic value, which justifies our reasoning above.

So far, we have concentrated on the analysis of the net quark and gluon contribution to the nucleon spin and the net quark contribution to the orbital angular momentum. Now, we try to make a flavor decomposition of the quark contribution to the nucleon spin and orbital angular momentum, which requires the knowledge of the quantity $B_{20}^{u-d}(0)$, i.e., the isovector nucleon AGM. Since we want to investigate the scale dependencies of the momentum fractions and the total angular momenta of the quarks and gluons up to $Q^2 = 4$ GeV^2, we use again the NLO evolution equation with three active flavors, although we assume that the strange quarks carry a negligible momentum fraction and AGM at the initial low-energy scale, for simplicity. As initial conditions of evolution, we need the following quantities at $Q^2 = 0.30$ GeV^2:

$$\langle x\rangle^{(0)} = \langle x\rangle^{u+d+s} \equiv \langle x\rangle^Q, \qquad \langle x\rangle^g, \tag{70}$$

$$\langle x\rangle^{(3)} = \langle x\rangle^{u-d}, \qquad \langle x\rangle^{(8)} = \langle x\rangle^{u+d-2s}. \tag{71}$$

The singlet moments $\langle x\rangle^Q$ and $\langle x\rangle^g$ evolve according to the evolution Eq. (57). Here, we use the initial condition

$$\langle x\rangle^{u+d} = 0.785, \qquad \langle x\rangle^{u-d} = 0.250, \qquad \langle x\rangle^g = 0.215, \tag{72}$$

with $\langle x\rangle^s = 0$, since it gives at $Q^2 = 4$ GeV^2

$$\langle x\rangle^{u+d+s} = 0.579, \qquad \langle x\rangle^g = 0.421, \tag{73}$$

$$\langle x\rangle^{u+d} = 0.552, \qquad \langle x\rangle^{u-d} = 0.158, \tag{74}$$

which approximately reproduces the empirical MRST2004 fit at the same scale [53]. We can make a similar analysis also for the total angular momentum of the quarks and gluons, because they obey the same evolution equations as the corresponding momentum fractions. To proceed, we need initial conditions for the following quantities:

$$J^{u+d} = \frac{1}{2}[\langle x\rangle^{u+d} + B_{20}^{u+d}(0)],$$
$$J^{u-d} = \frac{1}{2}[\langle x\rangle^{u-d} + B_{20}^{u-d}(0)],$$
$$J^{g} = \frac{1}{2}[\langle x\rangle^{g} + B_{20}^{g}(0)],$$

with the general constraint $B_{20}^{u+d}(0) + B_{20}^{g}(0) = 0$. Here, we have assumed $J_s = 0$ at the initial scale. For $B_{20}^{u+d}(0)$, we consider the two cases again, i.e.,$B_{20}^{u+d}(0) = 0$ and $B_{20}^{u+d}(0) = -0.12$. For $B_{20}^{u-d}(0)$, we use the prediction of the CQSM given by

$$B_{20}^{u-d}(0) = 0.458. \tag{75}$$

At first sight, the magnitude of the isovector AGM above seems to be fairly larger than the corresponding predictions of the lattice QCD given at $Q^2 = 4$ GeV^2. As already mentioned in the previous section, however, after taking account of the scale dependence, we find that the above CQSM prediction for $B_{20}^{u-d}(0)$ is remarkably close to that of the lattice QCD.

Now that all the necessary conditions are given at the initial scale $Q^2 = 0.30$ GeV^2, let us first try to estimate the total angular momentum fractions at $Q^2 = 4$ GeV^2, which correspond to the renormalization scale of lattice QCD simulations. First, we show the results corresponding to the choice $B_{20}^{u+d}(0) = 0$. We have, at $Q^2 = 4$ GeV^2,

$$\langle x\rangle^{Q} = 0.579, \qquad \langle x\rangle^{g} = 0.421, \tag{76}$$

$$\langle x\rangle^{u+d} = 0.552, \qquad \langle x\rangle^{u-d} = 0.158, \qquad \langle x\rangle^{s} = 0.028, \tag{77}$$

and

$$2J^{Q} = 0.579, \qquad 2J^{g} = 0.421, \tag{78}$$

$$2J^{u+d} = 0.552, \qquad 2J^{u-d} = 0.448, \qquad 2J^{s} = 0.028, \tag{79}$$

which gives

$$2J^{u} \simeq 0.500, \qquad 2J^{d} \simeq 0.052. \tag{80}$$

On the other hand, with the choice $B_{20}^{u+d}(0) = -0.12$ at the initial energy scale, we get

$$2J^{Q} = 0.519, \qquad 2J^{g} = 0.481, \tag{81}$$

$$2J^{u+d} = 0.486, \qquad 2J^{u-d} = 0.448, \qquad 2J^{s} = 0.033, \tag{82}$$

which gives

$$2J^{u} \simeq 0.467, \qquad 2J^{d} \simeq 0.019. \tag{83}$$

Depending on the two choices for $B_{20}^{u+d}(0)$. i.e., $B_{20}^{u+d}(0) \simeq -0.12$ or $B_{20}^{u+d}(0) = 0$, we thus obtain an estimate,

$$2J^{u} \simeq 0.46 - 0.50, \qquad 2J^{d} \simeq 0.02 - 0.05, \tag{84}$$

which supports the conclusion of the lattice QCD studies that the total angular momentum carried by the d-quarks is nearly zero at least qualitatively. For reference, we show in Fig. 5 the predicted scale dependence of J^u and J^d.

Now, the information on the quark OAM can be obtained from J^u, J^d, and J^s by subtracting the corresponding intrinsic spin contributions. Here, we use the empirical information provided by the recent HERMES analysis [9], which gives at $Q^2 = 5$ GeV^2,

$$g_A^{(0)} \equiv \Delta\Sigma^{u+d+s} = 0.330 \pm 0.011(\text{theor}) \pm 0.025(\text{exp}) \pm 0.028(\text{evol}), \tag{85}$$

$$g_A^{(3)} \equiv \Delta\Sigma^{u-d} = 1.269 \pm 0.003, \tag{86}$$

$$g_A^{(8)} \equiv \Delta\Sigma^{u+d-2s} = 0.586 \pm 0.031. \tag{87}$$

Neglecting the error-bars, for simplicity, this gives

$$\Delta\Sigma^{u} = 0.842, \qquad \Delta\Sigma^{d} = -0.427, \qquad \Delta\Sigma^{s} = -0.085. \tag{88}$$

As is well known, due to the conservation of the flavor nonsinglet axial-current, $g_A^{(3)}$ and $g_A^{(8)}$ are exactly scale independent. Then, if we neglect very weak scale depen-

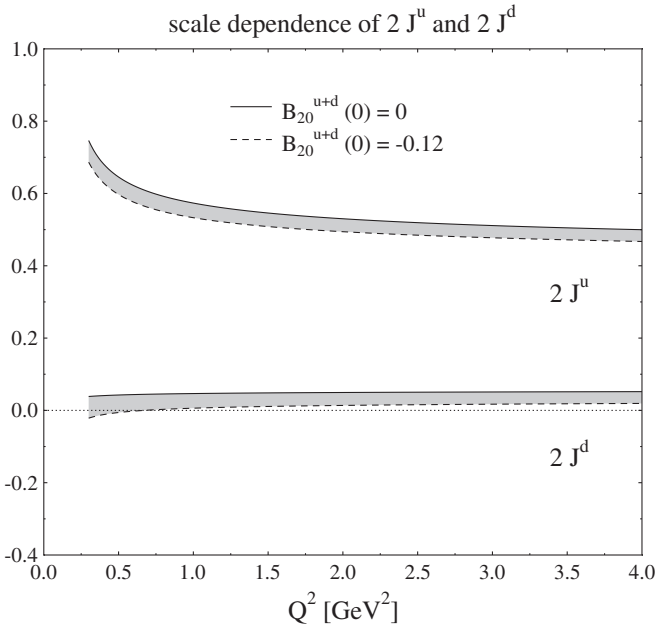

FIG. 5. The scale dependencies of J^u and J^d. The solid and dashed curves, respectively, correspond to the choices $B_{20}^{u+d}(0) = 0$ and $B_{20}^{u+d}(0) = -0.12$.

dence of $g_A^{(0)}$, all of $\Delta\Sigma^u$, $\Delta\Sigma^d$, and $\Delta\Sigma^s$ are thought to be scale independent. Let us first estimate the quark OAM at $Q^2 = 4$ GeV^2. Depending on the two choices for $B_{20}^{u+d}(0)$, i.e., $B_{20}^{u+d}(0) = -0.12$ and $B_{20}^{u+d}(0) = 0$, we obtain

$$\begin{aligned} 2L^u &= -(0.333 - 0.300), \\ 2L^d &= 0.489 - 0.522, \\ 2L^s &= 0.033 - 0.028. \end{aligned} \tag{89}$$

A prominent feature here is that the magnitudes of L^u and L^d are sizably large with the opposite sign such that $L^u < 0$ and $L^d > 0$, which leads to the inequality

$$|L^{u+d}| \ll |L^{u-d}|, \tag{90}$$

i.e., the *isovector dominance* of the quark OAM. (As already discussed, the cancellation between L^u and L^d is not so perfect in our semiphenomenological analysis as compared with the lattice QCD predictions.) To understand the physical meaning of the above unique feature, we find it instructive to look into the scale dependence of L^{u-d} as well as of L^u and L^d.

Shown in Fig. 6 are scale dependencies of $2L^u$, $2L^d$, and $2L^{u-d}$. (Note that the difference L^{u-d} of L^u and L^d does not depend on the choice of $B_{20}^{u+d}(0)$.) One clearly sees that L^{u-d} is a decreasing function of Q^2. Since L^{u-d} is negative, this means that $|L^{u-d}|$ is an increasing function of Q^2. Actually, this somewhat peculiar behavior of L^{u-d} can naturally be understood from the definitional equation of quark OAM:

$$2L^{u-d}(Q^2) \equiv 2J^{u-d}(Q^2) - \Delta\Sigma^{u-d}. \tag{91}$$

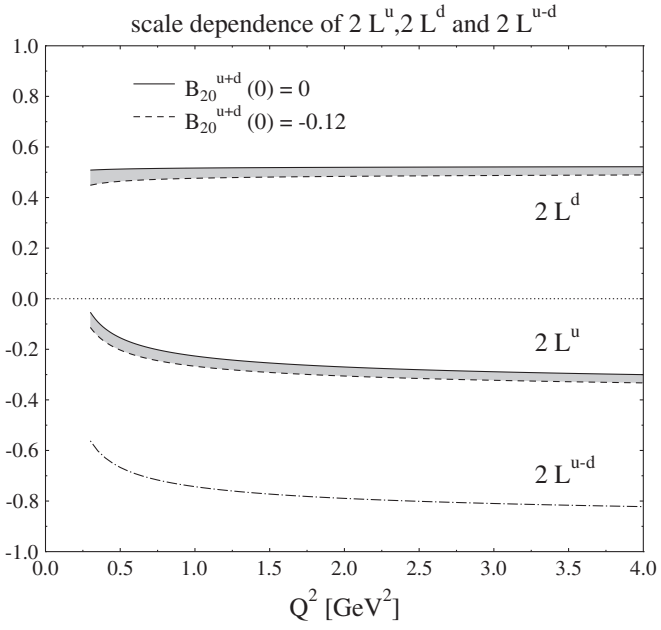

FIG. 6. The scale dependencies of L^u and L^d as well as L^{u-d}. The solid and dashed curves, respectively, correspond to the choices $B_{20}^{u+d}(0) = 0$ and $B_{20}^{u+d}(0) = -0.12$.

Since $J^{u-d}(Q^2)$ is a decreasing function of Q^2, while $\Delta\Sigma^{u-d}$ is Q^2-independent, $L^{u-d}(Q^2)$ is a decreasing function of Q^2. In particular, since $2J^{u-d}(\infty) = 0$, as verified from the nonsinglet evolution Eq. (63), one finds that the isovector quark OAM in the asymptotic limit $Q^2 \to \infty$ is solely determined by the isovector axial-charge of the nucleon $g_A^{(I=1)} \equiv \Delta\Sigma^{u-d}$ as

$$2L^{u-d}(\infty) = -g_A^{(I=1)} = -1.269. \tag{92}$$

This is really an astonishing observation, since it means that the quark OAM in the asymptotic limit, at least its isovector combination, is determined solely by the longitudinal quark polarization! Note that, since there is no room for doubt in using the relation $L^q = J^q - \frac{1}{2}\Delta\Sigma^q$ to extract quark OAM, this mysterious conclusion is an inevitable consequence of the following two theoretical postulates:

(i) the definition of J^q through Ji's angular momentum sum rule, $J^q = \frac{1}{2}[\langle x\rangle^q + B_{20}^q(0)]$.
(ii) the observation that J^q and $\langle x\rangle^q$ obey the same evolution equation.

Anyhow, since the net quark OAM $2L^{u+d}(Q^2)$ is a rapidly decreasing function of Q^2, we can easily understand the feature that L^u is large and negative, while L^d is large and positive above a few GeV scale. It is an interesting open question whether such a large OAM of the u- and d-quarks with opposite sign can be verified through some direct measurements like the single-spin asymmetry of semi-inclusive reactions depending on the Sivers mechanism [19], which is believed to be sensitive to the OAM of nucleon constituents.

Now, we attempt to give a complete solution to our first question, i.e., the problem of determining the full spin contents of the nucleon. Our answer on the decomposition of the nucleon spin into the sum of L^Q, $\frac{1}{2}\Delta\Sigma$, and J^g is already given in Fig. 4 within the range $0.30\ \text{GeV}^2 \lesssim Q^2 \lesssim 4.0\ \text{GeV}^2$. Still, uncompleted is further decomposition of J^g into the sum of Δg and L^g. Unfortunately, this decomposition is not gauge invariant and it cannot be done very reliably as compared with the analysis done so far. Still, the following qualitative consideration would be of some help to have a rough idea about the complete decomposition of the nucleon spin, thereby clarifying the fairly confused situation pointed out in the Introduction. A basis of the following analysis is the observation that the gluon polarization in the nucleon cannot be very large at least at the low renormalization scales [7,8] and HERMES groups [9]. As the simplest trial, we therefore assume that the gluon polarization Δg is zero, at the low-energy model scale around $Q^2 = 0.3$ GeV^2. Combining this with the CQSM prediction $\Delta\Sigma = 0.35$ for the net quark longitudinal polarization, we solve the NLO evolution equation for $\Delta\Sigma$ and Δg in the standard $\overline{\text{MS}}$ factorization scheme.

The resultant $\Delta\Sigma$ and Δg as functions of Q^2 are illustrated in Fig. 7 together with the empirical values obtained

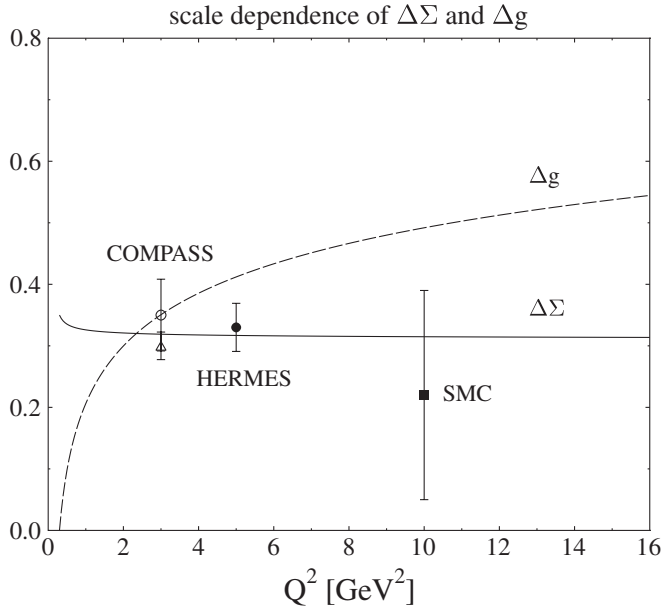

FIG. 7. The scale dependencies of $\Delta\Sigma$ and Δg, obtained as explained in the text, are compared with the recent QCD fits by the COMPASS group (open circle and open triangle) and by the HERMES group (filled circle). The old SMC result is also shown for reference by the filled square.

in the recent NLO analyses by the COMPASS and the HERMES groups [7–9], as well as the old SMC fit [61]. As repeatedly emphasized, the new COMPASS and the HERMES results for $\Delta\Sigma$ are remarkably close to the prediction of the CQSM. Also noteworthy here is the strong scale dependence of the longitudinal gluon polarization. In spite of that we have assumed that Δg is zero at the starting energy scale; it grows rapidly with increasing Q^2. As nicely explained in [62], the growth of the gluon polarization with Q^2 can be traced back to the positive sign of the relevant anomalous dimension $\delta\gamma_{qg}^{(0)1}$. The positivity of this quantity dictates that the polarized quark is preferred to radiate a gluon with helicity parallel to the quark polarization. Since the net quark spin component in the proton is clearly positive, it follows that $\Delta g > 0$ at least for the gluon perturbatively radiated from the quarks. The growth rate of Δg is so fast especially in the relatively low Q^2 region that its magnitude reaches around (0.3–0.4) already at $Q^2 = 3$ GeV^2, which may be compared with the estimate given by the COMPASS group:

$$\Delta g(Q^2 = 3\ \mathrm{GeV}^2)_{\mathrm{COMPASS}} \simeq (0.2\text{–}0.3). \qquad (93)$$

It should be emphasized that the gluon polarization of this size is not inconsistent with the GRSV standard scenario of the polarized PDF fit [63]. (Almost the same viewpoint was emphasized also in a recent bag model study of the gluon polarization [64].) Let us therefore proceed further by assuming that our estimate of Δg shown in Fig. 7 is not extremely far from the reality, which enables us to carry out a decomposition of J^g into Δg and L^g.

Figure 8 shows the gluon OAM L^g obtained in the above way, together with $2J^g$ and $2\Delta g$. One sees that the gluon OAM L^g is a rapidly decreasing function of Q^2. This feature naturally follows since $L^g = J^g - \Delta g$ and the increasing rate of Δg is much faster than that of J^g. Very interestingly, the magnitude of L^g in the vicinity $Q^2 \simeq 1$ GeV^2 turns out to be fairly close to zero. We are not sure whether this can be interpreted as giving support to Brodsky and Gardner's interpretation of the recent COMPASS observation of small single-spin asymmetry on the isoscalar deuteron target.

Anyhow, keeping in mind that the spin decomposition of the nucleon is highly scale dependent, our estimate at the scale $Q^2 \simeq 4$ GeV^2 can be summarized as follows. The net angular momentum fractions carried by the quarks and the gluons are $2J^Q \simeq 0.52 - 0.58$ and $2J^g \simeq 0.42 - 0.48$. The total angular momentum carried by the quarks can further be decomposed into the spin and OAM parts as $\Delta\Sigma \simeq 0.33$ and $2L^Q \simeq 0.19 - 0.25$. The decomposition of J^g into the sum of Δg and L^g is still very ambiguous. But, the standard scenario for the evolution of Δg indicates that the gluon total angular momentum of the order of $2J^g \simeq 0.42 - 0.48$ is a consequence of the cancellation of relatively large and positive Δg and negative gluon OAM with a little smaller magnitude.

Finally, we make a short comment on the recent extraction of the quark total angular momentum through the model-dependent GPD analyses of the semi-inclusive reactions. The first experimental result for the quark angular momentum was obtained by the HERMES Collaboration by studying the hard exclusive π^0 production on the transversely polarized hydrogen target [65]. Their results, corresponding to the average energy scale $Q^2 \simeq 2.5$ GeV^2, are

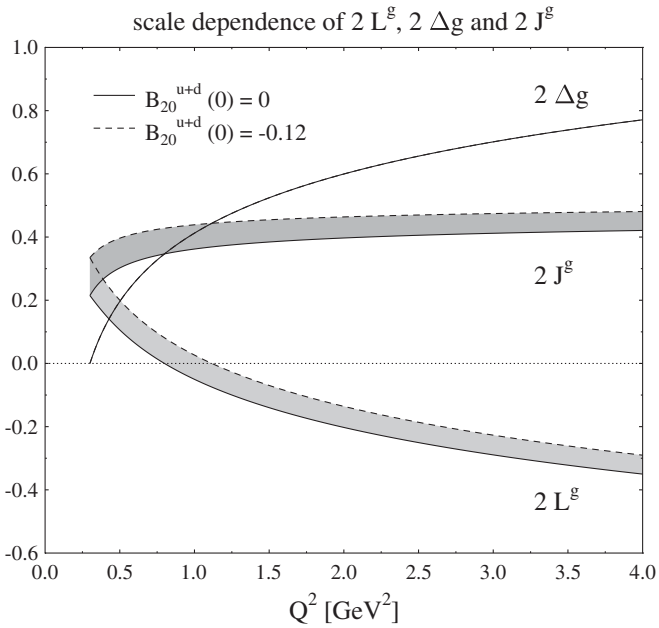

FIG. 8. The spin and OAM decomposition of gluon total angular momentum as a function of Q^2.

given by [66,67],

$$J^u + J^d/2.9 = 0.42 \pm 0.21 \pm 0.06. \tag{94}$$

On the other hand, another combination of J^u and J^d was extracted by the JLab Hall A Collaboration through the analysis of the DVCS and the Bethe-Heitler processes on the neutron and on the deuteron target [68]. Their result, corresponding to the average energy scale $Q^2 \simeq 1.9$ GeV^2, is given by

$$J^d + J^u/5.0 = 0.18 \pm 0.14. \tag{95}$$

For reference, we show below the corresponding predictions of our semiphenomenological analysis. Depending on the two choices $B_{20}^{u+d}(0) = -0.12$ and $B_{20}^{u+d}(0) = 0$, we obtain

$$J^u + J^d/2.9 = (0.245 - 0.268), \qquad Q^2 = 2.5 \text{ GeV}^2, \tag{96}$$

and

$$J^d + J^u/5.0 = (0.056 - 0.078), \qquad Q^2 = 1.9 \text{ GeV}^2. \tag{97}$$

Clearly, our estimates lie in the allowed ranges of both the HERMES and JLab determinations of J^u and J^d. However, it is also clear that the error-bars of the two determinations are still too large to be able to say something definite.

V. CONCLUDING REMARKS

After completing our semiempirical analysis of the nucleon spin contents, we now try to answer several questions raised in the Introduction. Accepting the observation that the intrinsic quark spin carries about $1/3$ of the total nucleon spin, what carries the rest of it? As we have shown, the answer depends on the scale of observation in an essential manner. At the relatively high-energy scale around $Q^2 \simeq 4$ GeV^2, corresponding to the renormalization scale of the recent lattice QCD simulations, the quarks and gluons, respectively, carry about $(52 - 58)\%$ and $(0.42–0.48)\%$ of the total nucleon spin. The total angular momentum fraction $2J^Q$ carried by the quarks can further be decomposed into the spin and OAM parts as $\Delta\Sigma \simeq 0.33$ and $2L^Q \simeq 0.19 - 0.25$. Our estimate for the quark OAM appears to contradict the conclusion of the lattice QCD studies that the OAM carried the quarks is nearly zero. The cause of this discrepancy can mainly be traced back to a little overestimation of the net longitudinal quark polarization $\Delta\Sigma$ in the lattice QCD simulation. In fact, once we accept the use of the central value $\Delta\Sigma = 0.33$ given by the recent HERMES fit, the quark OAM of the order of 20% at $Q^2 \simeq 4$ GeV^2 is not unreasonable as can be shown from the following two observations based on the evolution equations of relevant quantities. One is the fact that the asymptotic ($Q^2 \to \infty$) value of the net quark OAM fraction is given by $2L^Q(\infty) = 2J^Q(\infty) - \Delta\Sigma \simeq 0.529 - 0.33 \simeq 0.199$ for $n_f = 6$. The other is the fact that L^Q is a decreasing function of Q^2. The decomposition of J^g into the sum of the spin and the OAM parts is still very ambiguous. Nonetheless, the standard scenario for the evolution of Δg strongly indicates that the total gluon angular momentum of the order $2J^g = 0.42 - 0.48$ at $Q^2 = 4$ GeV^2 is likely to be a consequence of the cancellation of relatively large and positive Δg and negative gluon OAM with a little smaller magnitude.

At the low-energy scales of nonperturbative QCD around $Q^2 \simeq (0.30 - 0.70)$ GeV^2, we get a very different picture on the nucleon spin contents. In these energy scales, the quark OAM, the intrinsic quark spin, and the gluon total angular momentum would give roughly the same magnitude of contributions to the nucleon spin, i.e., $2L^Q \simeq \Delta\Sigma \simeq 2J^g \simeq 1/3$.

Also very interesting is the flavor decomposition of the total angular momentum and the OAM carried by the quarks. On the basis of Ji's observation that J^q and $\langle x \rangle^q$ obey the same evolution equation, we have shown that the asymptotic limit of the isovector quark OAM is *solely* determined by the isovector axial-charge of the nucleon or the isovector part of the longitudinal quark polarization as $2L^{u-d}(\infty) = -g_A^{(I=1)} = -\Delta\Sigma^{u-d} = -1.269$, which leads to novel *isovector dominance* of the quark OAM at the high-energy scale. It is an interesting open question whether this unique feature of the quark OAM at high Q^2 can be probed through some direct observations in high-energy DIS processes.

ACKNOWLEDGMENTS

This work is supported in part by a Grant-in-Aid for Scientific Research from the Ministry of Education, Culture, Sports, Science and Technology, Japan (No. C-16540253)

[1] J. Ashman *et al.* (EMC Collaboration), Phys. Lett. B **206**, 364 (1988).
[2] J. Ashman *et al.* (EMC Collaboration), Nucl. Phys. **B328**, 1 (1989).
[3] E. S. Ageev *et al.* (COMPASS Collaboration), Phys. Lett. B **633**, 25 (2006).
[4] K. Boyle *et al.* (PHENIX Collaboration), AIP Conf. Proc. **842**, 351 (2006).

[5] J. Kiryluk *et al.* (STAR Collaboration), AIP Conf. Proc. **842**, 327 (2006).
[6] R. Fatemi *et al.* (STAR Collaboration), arXiv:nucl-ex/0606007.
[7] E. S. Ageev *et al.* (COMPASS Collaboration), Phys. Lett. B **612**, 154 (2005).
[8] V. Yu. Alexakhin *et al.* (COMPASS Collaboration), Phys. Lett. B **647**, 8 (2007).
[9] A. Airapetian *et al.* (HERMES Collaboration), Phys. Rev. D **75**, 012007 (2007).
[10] M. Göckeler, R. Horsley, D. Pleiter, P. E. L. Rakow, A. Schäfer, G. Schierholz, and W. Schroers. (QCDSF Collaboration), Phys. Rev. Lett. **92**, 042002 (2004).
[11] M. Göckeler, T. R. Hemmert, R. Horsley, D. Pleiter, P. E. L. Rakow, A. Schäfer, G. Schierholz, and W. Schroers (QCDSF Collaboration), Nucl. Phys. B, Proc. Suppl. **128**, 203 (2004).
[12] Ph. Hägler, J. W. Negele, D. B. Renner, W. Schroers, Th. Lippert, and K. Schlling. (LHPC and SESAM Collaboration), Phys. Rev. D **68**, 034505 (2003).
[13] Ph. Hägler, J. W Negele, D. B. Renner, W. Schroers, Th. Lippert, and K. Schilling (LHPC and SESAM Collaboration), Phys. Rev. Lett. **93**, 112001 (2004).
[14] J. W. Negele *et al.* (LHPC Collaboration), Nucl. Phys. B, Proc. Suppl. **128**, 170 (2004).
[15] Ph. Hägler, J. W Negele, D. B. Renner, W. Schroers, Th. Lippert, and K. Schilling (LHPC Collaboration), Eur. Phys. J. A **24**, 29 (2005).
[16] D. Dolgov *et al.* (LHPC-SESAM Collaboration), Phys. Rev. D **66**, 034506 (2002).
[17] Ph. Hägler *et al.* (LHPC Collaboration), arXiv:0705.4295.
[18] D. Brömmel *et al.* (QCDSF-UKQCD Collaboration), Proc. Sci. LAT2007 (**2007**) 158.
[19] D. W. Sivers, Phys. Rev. D **41**, 83 (1990); **43**, 261 (1991).
[20] M. Burkardt, Phys. Rev. D **66**, 114005 (2002).
[21] S. J. Brodsky and S. Gardner, Phys. Lett. B **643**, 22 (2006).
[22] V. Y. Alexakhin *et al.* (COMPASS Collaboration), Phys. Rev. Lett. **94** 202002 (2005).
[23] X. Ji, Phys. Rev. Lett. **78**, 610 (1997).
[24] P. Hoodbhoy, X. Ji, and W. Lu, Phys. Rev. D **59**, 014013 (1998).
[25] X. Ji, J. Tang, and P. Hoodbhoy, Phys. Rev. Lett. **76**, 740 (1996).
[26] X. Ji, J. Phys. G **24**, 1181 (1998).
[27] M. Wakamatsu and Y. Nakakoji, Phys. Rev. D **74**, 054006 (2006).
[28] K. Goeke, J. Grabis, J. Ossmann, M. V. Polyakov, P. Schweitzer, A. Silva, and D. Urbano, Phys. Rev. C **75**, 055207 (2007).
[29] K. Goeke, J. Grabis, J. Ossmann, M. V. Polyakov, P. Schweitzer, A. Silva, and D. Urbano, Phys. Rev. D **75**, 094021 (2007).
[30] K. Goeke, J. Ossmann, P. Schweitzer, and A. Silva, Eur. Phys. J. A **27**, 77 (2006).
[31] M. Wakamatsu, Phys. Rev. D **72**, 074006 (2005).
[32] M. Wakamatsu and T. Watabe, Phys. Lett. B **312**, 184 (1993).
[33] C. V. Christov, A. Blotz, K. Goeke, P. Pobylitsa, V. Yu. Petrov, M. Wakamatsu, and T. Watabe, Phys. Lett. B **325**, 467 (1994).
[34] M. Wakamatsu, Prog. Theor. Phys. **95**, 143 (1996).
[35] S. Kahana and G. Ripka, Nucl. Phys. **A429**, 462 (1984).
[36] S. Kahana, G. Ripka and V. Soni, Nucl. Phys. **A415**, 351 (1984).
[37] M. Wakamatsu and H. Yoshiki, Nucl. Phys. **A524**, 561 (1991).
[38] T. Kubota, M. Wakamatsu, and T. Watabe, Phys. Rev. D **60**, 014016 (1999).
[39] M. Wakamatsu and T. Kubota, Phys. Rev. D **60**, 034020 (1999).
[40] M. Wakamatsu, Phys. Rev. D **67**, 034005 (2003); **67**, 034006 (2003).
[41] M. Wakamatsu, Phys. Rev. D **71**, 057504 (2005).
[42] O. V. Teryaev, arXiv:hep-ph/9803403.
[43] O. V. Teryaev, AIP Conf. Proc. **915**, 260 (2007).
[44] J. Ossmann, M. V. Polyakov, P. Schweitzer, D. Urbano, and K. Goeke, Phys. Rev. D **71**, 034011 (2005).
[45] M. Wakamatsu and H. Tsujimoto, Phys. Rev. D **71**, 074001 (2005).
[46] K. Goeke, M. V. Polyakov, and M. Vanderhaegen, Prog. Part. Nucl. Phys. **47**, 401 (2001).
[47] M. Glück, E. Reya, and A. Vogt, Z. Phys. C **67**, 433 (1995).
[48] M. Glück, E. Reya, M. Strattmann, and W. Vogelsang, Phys. Rev. D **53**, 4775 (1996).
[49] T. Weigl and W. Melnitchouk, Nucl. Phys. **B465**, 267 (1996).
[50] E. G. Floratos, D. A. Ross, and C. T. Sachrajda, Nucl. Phys. **B129**, 66 (1977).
[51] C. Lopéz and F. J. Ynduráin, Nucl. Phys. **B183**, 157 (1981).
[52] K. Adel, F. Barreiro, and F. J. Ynduráin, Nucl. Phys.**B495**, 221 (1997).
[53] A. D. Martin, W. J. Stirling, and R. S. Thorne, Phys. Lett. B **636**, 259 (2006).
[54] L. H. Lai, J. Huston, S. Kuhlmann, J. Morfin, F. Olness, J. F. Owen, J. Pumplin, and W. K. Tung, Eur. Phys. J. C **12**, 375 (2000).
[55] H. Weigel, L. Gamberg, and H. Reinhardt, Mod. Phys. Lett. A **11**, 3021 (1996).
[56] L. Gamberg, H. Reinhardt, and H. Weigel, Phys. Rev. D **58**, 054014 (1998).
[57] D. I. Diakonov, V. Yu. Petrov, P. V. Pobylitsa, M. V. Polyakov, and C. Weiss, Nucl. Phys. **B480**, 341 (1996).
[58] D. I. Diakonov, V. Yu. Petrov, P. V. Pobylitsa, M. V. Polyakov, and C. Weiss, Phys. Rev. D **56**, 4069 (1997).
[59] O. V. Teryaev, arXiv:hep-ph/9904376.
[60] M. Wakamatsu and T. Watabe, Phys. Rev. D **62**, 054009 (2000).
[61] B. Adeva *et al.* (SMC Collaboration), Phys. Rev. D **58**, 112001 (1998).
[62] H.-Y. Cheng, Phys. Lett. B **427**, 371 (1998).
[63] M. Glück, E. Reya, M. Stratmann, and W. Vogelsang, Phys. Rev. D **63**, 094005 (2001).
[64] P. Chen and X. Ji, Phys. Lett. B **660**, 193 (2008).
[65] F. Ellinghaus, W.-D. Nowak, and A. V. Vinnikov, Eur. Phys. J. C **46**, 729 (2006).
[66] F. Ellinghaus, arXiv:0710.5768.
[67] Z. Ye, arXiv:hep-ex/0606061.
[68] M. Mazous *et al.* (JLab Hall A Collaboration), Phys. Rev. Lett. **99**, 242501 (2007).